

Kinetic Analysis of the Temperature Dependence of the Template-Directed Formation of Oligoguanylate from the 5′-Phosphorimidazolide of Guanosine on a Poly(C) Template with Zn^{2+}

Kunio Kawamura* **and Masatosi Umehara**

Department of Applied Chemistry, Osaka Prefecture University, Sakai, Osaka 599-8531

(Received October 3, 2000)

A kinetic study of the temperature dependence of the template-directed formation of oligoguanylate (oligo(G)) on polycytidylic acid (poly(C)) from the 5′-phosphorimidazolide of guanosine (ImpG) has been carried out in the presence of Zn^{2+} at 40–80 °C. It is surprising that a large amount of oligo(G) was formed at 40–60 °C and a small amount of oligo(G) was detected even at 80 °C. The rate constants of the template-directed formation of oligo(G) were determined at 40–60 °C, and the same trend, the rate constants increase with the chain length, was observed as that at lower temperatures. Besides, second-order rate plots of the hydrolyses of ImpG and oligo(G) were consistent with pseudo-second-order processes in the presence of 0.04 M Zn^{2+}. The apparent activation energy determined from the Arrhenius plots decreases in the order hydrolysis of oligo(G) > formation of 4-mer ≈ formation of 3-mer ≈ hydrolysis of ImpG > formation of 2-mer. The kinetic analysis and computer simulations demonstrate the importance of the rate of 2-mer formation to determine the efficiency of the oligo(G) formation.

The discovery of the catalytic activity of RNA suggests that RNA or RNA-like molecules had a central role on the primitive earth.[1–5] If the RNA world hypothesis is correct, then RNA-like molecules formed spontaneously under primitive earth conditions. A number of successful studies of relevance with the RNA world hypothesis have been carried out.[6–10]

On the other hand, it is widely believed that hydrothermal systems, such as hydrothermal vents in the deep ocean, played an important role for the prebiotic synthesis of biologically essential molecules.[11–20] Based on the discovery of thermophilic organisms in association with hydrothermal conditions, it has been deduced that life on earth might have originated in hydrothermal systems.[21–26] This hypothesis has been supported by phylogenetic analyses of modern microorganisms, which suggest that the last common ancestor (LCA) was a hyperthermophile. Besides, there has been a challenging proposal on LCA that was not a hyperthermophilic organism.[27] Despite much effort towards LCA, the nature of LCA is still unclear.[28]

In contrast to the importance of hydrothermal prebiotic synthesis, the rapid disappearance of prebiotic molecules suggests that the emergence of primitive organisms at high temperatures was difficult.[29–35] For example, although it is generally considered that RNA is unstable under hydrothermal conditions, there has been fewer systematic studies on the stability of RNA at high temperatures.[34,35] Thus, we have been studying the stability of RNA molecules in aqueous solution at high temperatures.[36–41] The experiments have provided quantitative data that nucleotides are notably unstable in aqueous solution at high temperatures. Although this fact may support that the emergence of the RNA world was not possible in hydrothermal systems, the accumulation of RNA molecules in the RNA world should be determined by both the rates of the formation and the decomposition of RNA. Thus, parallel investigations on the kinetics of the temperature dependence of the prebiotic formation and decomposition of RNA are important to evaluate the RNA world hypothesis from the viewpoint of hydrothermal reactions.

There have been a number of successful studies of the condensation reaction of activated nucleotides to form RNA oligonucleotides in the presence[42–45] and absence of RNA templates.[46–50] However, the experiments have only been carried out at temperatures up to 37 °C.[51] Thus, it is important to investigate the scope of these successful studies at higher temperatures. That is to say, a kinetic analysis of the temperature dependence of the template-directed synthesis could explore the knowledge on the prebiotic chemistry of RNA.[52]

Besides, a variety of kinetic investigations of prebiotic synthesis of oligonucleotides have been carried out to provide insight into the mechanism of oligonucleotide formation on RNA templates[53–59] and montmorillonite clay catalysts.[60,61] Thus, a kinetic analysis of the prebiotic formation of RNA at elevated temperatures would provide a basis to know whether the chemical evolution of RNA has occurred under hydrothermal environments or not. However, there has been no kinetic analysis on the condensation of activated nucleotide in the presence and absence of templates at temperatures higher than 23 °C.[53–59] In this study, the kinetics of the formation of oligo(G) from the poly(C)-template-directed reaction in the presence of Zn^{2+} [62–64] was investigated at 40–80 °C. The rate constants of the formation of oligo(G) and those of the hydrolyses of oligo(G) and ImpG were determined. Based on a comparison between the rates of the formation and the decomposition of oligo(G), it was deduced that both the rates of the formation of 2-mer and the decomposition of oligo(G) are important fac-

tors to determine the yield of long oligonucleotides. Further, kinetic simulations were performed to visualize the importance of 2-mer formation. Based on the results, the reason for the difficulty regarding template-directed formation of oligo(G) in hydrothermal environments is going to be discussed.

Experimental

Materials and Equipment. ImpG was synthesized using a modification of the procedure of Joyce et al. (purity 97%).[65,66] Polycytidylic acid (poly(C)), ribonuclease A (RNase A), ribonuclease T_1 (RNase T_1), ribonuclease T_2 (RNase T_2), and P_1,P_2-bis(5′-guanosyl)diphosphate ($G^{5'}$ppG) were purchased from SIGMA. All other reagents used were of analytical grade.

High-performance liquid chromatography (HPLC) was performed by a HPLC system LC10A (Shimadzu, Japan) with a DNA-NPR anion-exchange column from TOSOH Co., Japan using a gradient of 0.3–1.5 M (1 M = 1 mol dm^{-3}) NaCl at pH 11 with 0.02 M 2-amino-2-hydroxymethyl-1,3-propanediol (Tris) buffer and a ODS-2 column from GL Science Co., Japan using a gradient of 0.005 M NaH_2PO_4 in water at pH 3.5 mixed with 0.01 M NaH_2PO_4 in 40% CH_3OH at pH 4.0.

Kinetic Measurements. Oligomerization of ImpG on Poly(C) Template at Elevated Temperatures. The template-directed formation of oligo(G) on a poly(C) template from ImpG was performed in a solution containing 0.015 M ImpG, 0.025 M poly(C), 1 M NaCl, 0.2 M $MgCl_2$, 0.1 M 2-[4-(2-hydroxyethyl)-1-piperazinyl]ethanesulfonic acid (HEPES), 0.04 M $ZnCl_2$, at pH 8.0. A 200 μL of the ImpG solution was added to a 500 μL plastic vial with a screw cap, which bears up to 120 °C, and the vial was settled to a cartridge heater controlled at 40–80 °C. The reaction was monitored at regular intervals over 24 h and the sample solution was immediately quenched in liquid nitrogen at the end of the reaction.

The sample was incubated with RNase A to cleave poly(C) in the presence of a 0.1 M EDTA solution to mask Zn^{2+}. RNase A hydrolysis was performed in 0.1 mL of the reaction mixture for 18 h at 37 °C using 300 units. The sample was analyzed by the anion-exchange and the reversed-phase HPLC. The hypochromicity correction factor was regarded as approximately 1 under the HPLC conditions.[53] The extent of 3′,5′-linked oligo(G) was determined using RNase T_2 or RNase T_1. The hydrolysis with RNase T_2 was carried out in 0.1 mL of the sample solution for 18 h at 37 °C using 30 units, and that with RNase T_1 was performed in 0.1 mL for 18 h at 37 °C using 200 units of enzyme. The extent of oligo(G)s was determined based on anion-exchange HPLC and reversed-phase HPLC analyses.

Hydrolysis of ImpG. The rates of ImpG hydrolysis were determined in a solution containing 0.015 M ImpG, 1M NaCl, 0.2 M $MgCl_2$, 0.1 M HEPES, 0.04 M, or 0.004 M $ZnCl_2$ at pH 8.0. The hydrolysis reaction was monitored for 24 h and the samples were analyzed by reversed-phase HPLC.

Hydrolysis of Oligo(G). A standard solution containing oligo(G) was prepared from the incubation of poly(G) in 0.1 M NaOH for 40 min at 37 °C and the treatment in 1 M $HClO_4$ to cleave 2′,3′-cyclic phosphate.[42] The mixture was neutralized with NaOH solution to avoid any further hydrolysis of oligo(G).

The hydrolysis of standard oligo(G) was monitored in a solution containing 1 M NaCl, 0.2 M $MgCl_2$, 0.1 M HEPES, 0.04 M $ZnCl_2$, at pH 8.0 in the presence of 0.025 M poly(C) for 144 h at 60–100 °C. At regular time intervals, an aliquot of the sample solution was withdrawn and immediately quenched in liquid nitrogen to stop further hydrolysis. The rates of the oligo(G) hydrolysis were followed in the absence and presence of a poly(C) template.

T_m Studies of ImpG, 5′-GMP, and Oligo(G) with Poly(C). The absorption spectra in a solution containing the same electrolytes as used in the kinetic investigations were determined using a Shimadzu UV-2500PC. The oligo(G) solution was prepared by the same procedure as used for the hydrolytic study of oligo(G).

Determination of Rate Constants and Kinetic Simulation. The computer program SIMFIT was used to evaluate the rate constants and the kinetic simulations of the template-directed formation of oligo(G).[9]

Results

Hydrolysis of ImpG in the Presence of Zn^{2+}. The hydrolysis of ImpG was investigated in the presence of Zn^{2+} to determine if it followed pseudo-first- or second-order kinetics. Because the hydrolysis of adenosine 5′-triphosphate obeys pseudo-second-order kinetics in the presence of several kinds of metal ions[67,68] it is plausible that the ImpG hydrolysis obeys pseudo-second-order kinetics. A hydrolysis study was carried out in the presence of 0.004 M and 0.04 M Zn^{2+} at 40–80 °C. The reaction curves are shown in Fig. 1, in which a small amount of $G^{5'}$ppG is observed. The first-order rate plots of the disappearance of ImpG were not best fitted at 0.04 M Zn^{2+} (Fig. 2a), while the hydrolysis of ImpG at 0.004 M Zn^{2+} was consistent with a pseudo-first-order process. Besides, the second-order rate plots were well fitted for the disappearance of ImpG at 0.04 M Zn^{2+} (Fig. 2b). Although detail analyses should be necessary to determine the reaction mechanism, these facts indicate that the hydrolysis mainly involves a second-order rate process at 0.04 M Zn^{2+}. Thus, the rate constants were determined on the basis of a pseudo-second-order model by SIMFIT. The rate constants of the ImpG hydrolysis and the formation of $G^{5'}$ppG from ImpG are summarized in Table 1. A best fit was obtained using a pseudo-second-order model, in which the sum of the errors was a few-times smaller than that obtained using a first-order model. The half-lives of ImpG, calculated from the rate constants shown in Table 1,

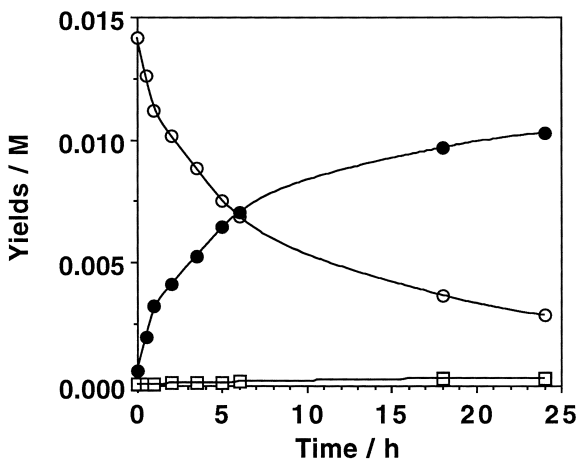

Fig. 1. Reaction curves for the hydrolysis of ImpG in the presence of Zn^{2+}. [NaCl] = 1.0 M, [$MgCl_2$] = 0.2 M, [HEPES] = 0.1 M, [$ZnCl_2$] = 0.04 M, [ImpG] = 0.015 M, pH = 8.0, 40 °C. Lines, ○, ImpG; ●, pG; □ , $G^{5'}$ppG.

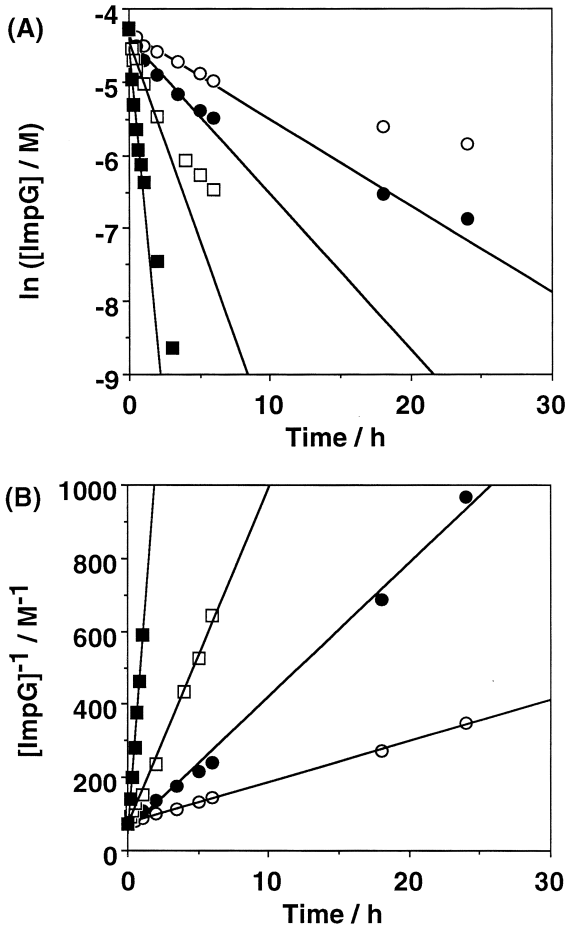

Fig. 2. (A) Pseudo-first-order rate plots and (B) pseudo-second-order rate plots for the hydrolysis of ImpG in the presence of Zn^{2+}. [NaCl] = 1.0 M, [$MgCl_2$] = 0.2 M, [HEPES] = 0.1 M, [$ZnCl_2$] = 0.04 M, [ImpG] = 0.015 M, pH = 8.0. Lines, ○, 40 °C; ●, 50 °C; □, 60 °C; ■, 80 °C.

Table 1. The Rate Constants for the ImpG Hydrolysis in the Presence of Zn^{2+} a)

T/°C	k_{hy}/s^{-1} M^{-1} b)	$kG^{5'}ppG$/s^{-1} M^{-1} c)
40	$(3.09 \pm 0.06) \times 10^{-3}$	$(1.09 \pm 0.26) \times 10^{-4}$
50	$(8.14 \pm 0.14) \times 10^{-3}$	$(2.33 \pm 0.45) \times 10^{-4}$
60	$(2.62 \pm 0.14) \times 10^{-2}$	$(1.28 \pm 0.42) \times 10^{-3}$
80	$(1.04 \pm 0.01) \times 10^{-1}$	$(4.06 \pm 0.42) \times 10^{-3}$

a) Reactions were performed in a solution containing 0.015 M ImpG, 0.04 M $ZnCl_2$, 1.0 M NaCl, 0.2 M $MgCl_2$, and 0.1 M HEPES at pH 8.0. The rate constants were determined using SIMFIT. The reaction curves were fitted by pseudo-second-order rate model. b) The rate constants for the hydrolysis of ImpG. c) The rate constants for the formation of $G^{5'}ppG$.

were 22 min at 60 °C and 5.6 min at 80 °C in the presence 0.04 M Zn^{2+}, while those were 3.1 h at 60 °C and 53 min at 80 °C in the presence of 0.004 M Zn^{2+}. This fact indicates that the hydrolysis of ImpG at 0.04 M Zn^{2+} was about 9-times more accelerated than that at 0.004 M Zn^{2+}. The apparent activation energy for the hydrolysis of ImpG determined from the Arrhenius plots is 82 kJ mol^{-1} at 0.04 M Zn^{2+} and 62 kJ mol^{-1} at 0.004 M Zn^{2+}.

Kinetics of the Oligomerization of ImpG at 40–80 °C. The reactions at 40 and 50 °C yielded oligo(G)s longer than 30-mer, and those at 60 and 80 °C yielded oligo(G)s longer than 20-mer (Figs. 3a–d). The high efficiency of the oligo(G) formation at elevated temperatures is unexpected, since 15–20-mer was the longest at 37 °C in a previous study.[51] The extent of ImpG, 5′-GMP, and $G^{5'}ppG$ in the monomer fraction on anion-exchange HPLC was determined on the basis of an analysis by reversed-phase HPLC, in which the total extent of 4-mer and longer oligomers was calculated at 40–80 °C (Fig. 4). The reaction curve at 60 °C indicates that the oligo(G) formed from ImpG was hydrolyzed after the template-directed formation of oligo(G). Because the yield of oligo(G)s was notably low at 80 °C, kinetic analyses were carried out at 40–60 °C.

The regioselectivity of 3′,5-phosphodiester bond formation was investigated by selective enzymatic hydrolysis with RNase T_1 and RNase T_2 (Table 2). The regioselectivity at 40–60 °C is consistent with that at lower temperature;[63] this fact indicates that the regioselectivity is not very sensitive at 0–60 °C.

The reaction curves of the disappearance of ImpG and the formation of oligo(G) at 40–60 °C were fitted by SIMFIT using the reaction pathways defined in Eq. I-1–5 by varying the pseudo-second-order rate constants. The reaction model is basically the same as that previously applied, except for using the second-order hydrolysis model of ImpG,[53,60,61] where subscript "n" designates the length of oligo(G).

$$2\,\mathrm{ImpG} \rightarrow \mathrm{ImpG} + \mathrm{pG} \quad \text{(I-1)}$$
$$\mathrm{ImpG} + \mathrm{pG} \rightarrow (\mathrm{pG})_2 \quad \text{(I-2)}$$
$$\mathrm{ImpG} + (\mathrm{pG})_2 \rightarrow (\mathrm{pG})_3 \quad \text{(I-3)}$$
$$\mathrm{ImpG} + (\mathrm{pG})_3 \rightarrow (\mathrm{pG})_4 \quad \text{(I-4)}$$
$$\cdots$$
$$\mathrm{ImpG} + (\mathrm{pG})_{n-1} \rightarrow (\mathrm{pG})_n \quad \text{(I-5)}$$

The rate constants were determined by continuous iteration to a convergent result using SIMFIT, in which a constant magnitude of k_4–k_n was defined as that postulated in previous studies.[58,59] The rate constants at 40–60 °C are summarized in Table 3.

Kinetics of Oligo(G) Hydrolysis. The reaction curves of the oligo(G) formation in the presence of a poly(C) template indicate that the hydrolysis of oligo(G) occurs after 6 h at 60 °C (Fig. 4). In order to evaluate the importance of the oligo(G) hydrolysis, the kinetics of the oligo(G) hydrolysis in both the presence and absence of poly(C) was studied at 60–100 °C.

Table 2. The Extent (%) of 3′,5′-Linked Oligonucleotides Formed from ImpG Condensation on Poly(C) Template in the Presence of $ZnCl_2$

T/°C	RNase T_1 a)	RNase T_1 b)	RNase T_2
40	95	96	83
50	95	96	90
60	95	98	90

a) No treatment before enzymatic hydrolysis. b) Samples with heating 1 min at 90 °C prior to enzymatic hydrolysis.

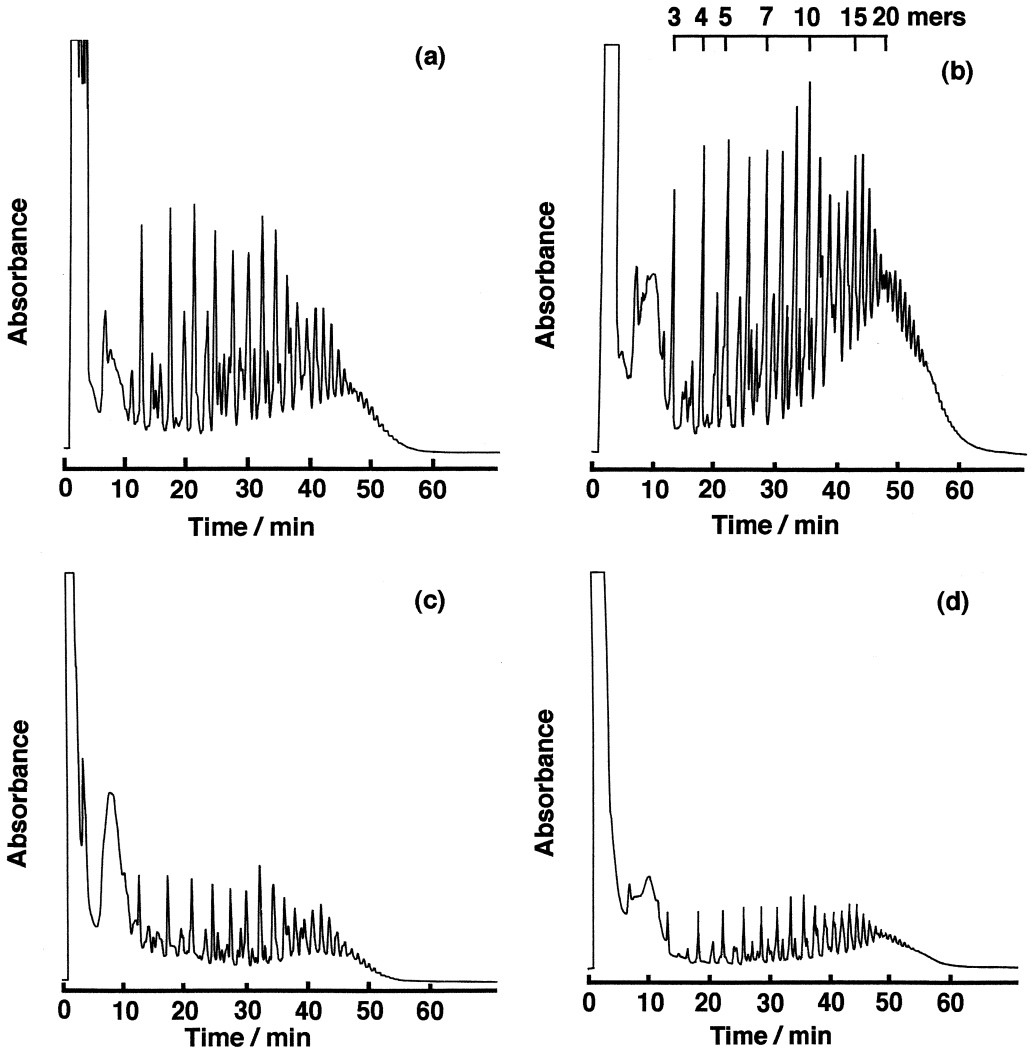

Fig. 3. HPLC profile of the template-directed formation of oligo(G) from ImpG on poly(C) template. [NaCl] = 1.0 M, [$MgCl_2$] = 0.2 M, [HEPES] = 0.1 M, [$ZnCl_2$] = 0.04 M, [ImpG] = 0.015 M, [poly(C)] = 0.025 M, pH = 8.0. (a), 40 ˚C, 6h; (b), 50 ˚C, 6 h; (c), 60 ˚C, 6 h; (d), 80 ˚C, 10 min.

Table 3. The Rate Constants (s^{-1} M^{-1}) for the ImpG Condensation at Elevated Temperatures[a)]

Length of oligo(G)	40 ˚C	50 ˚C	60 ˚C
2	$(1.19 \pm 0.06) \times 10^{-3}$	$(1.65 \pm 0.11) \times 10^{-3}$	$(2.77 \pm 0.16) \times 10^{-3}$
3	$(6.17 \pm 0.37) \times 10^{-2}$	$(1.96 \pm 0.18) \times 10^{-1}$	$(3.35 \pm 0.26) \times 10^{-1}$
average 4 <	$(9.11 \pm 0.42) \times 10^{-2}$	$(2.61 \pm 0.17) \times 10^{-1}$	$(6.45 \pm 0.55) \times 10^{-1}$

a) Reaction conditions are the same as shown in Table 1. The rate constants were determined using SIMFIT.

The rate of the oligo(G) hydrolysis was followed by the described procedure.[37] Oligo(G)s up to approximately 20-mer in length, which correspond to moderate oligo(G)s in length formed by the template-directed reaction, were prepared by the alkaline hydrolysis of poly(G) (described in the experimental section). The number of phosphodiester bonds remaining in oligo(G) was followed at regular time intervals during oligo(G) hydrolysis. The value (*N*), which is proportional to the number of phosphodiester bonds and normalized as being 100 at time 0, was determined during oligo(G) hydrolysis and the time courses of the *N* value were monitored (Fig. 5).[37] The reaction curves indicate that the hydrolysis of oligo(G) was notably inhibited in the presence of a poly(C) template, even at 100 ˚C. Further, the hydrolysis did not obey the pseudo-first-order rate, while the pseudo-second-order rate plots gave a good fit. Thus, the rate constants were determined on the basis of pseudo-second order kinetics by SIMFIT (Table 4).

In addition, the half-life of the degradation of the oligo(G) formed by the template-directed reaction at 60 ˚C is 15 h (Fig. 4), which is similar to that of oligo(G) in the absence of poly(C) ($t_{1/2}$ = 13 h), while $t_{1/2}$ in the presence of poly(C) is 130 h.

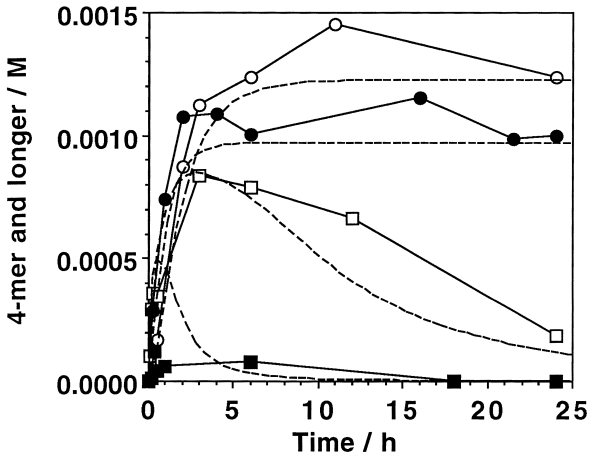

Fig. 4. The time course of the total amount of oligo(G) 4-mer and longer. [NaCl] = 1.0 M, [$MgCl_2$] = 0.2 M, [HEPES] = 0.1 M, [$ZnCl_2$] = 0.04 M, [ImpG] = 0.015 M, [poly(C)] = 0.025 M, pH = 8.0. plots and solid lines, ○, 40 °C; ●, 50 °C; □, 60 °C; ■, 80 °C. The dashed lines were reproduced by the simulation using Eq. II-1–6.

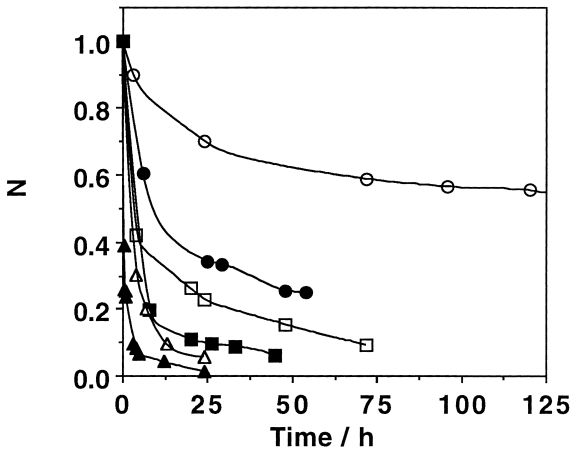

Fig. 5. The reaction curves of the disappearance of phosphodiester bond of oligo(G) in the presence and absence of poly(C). [NaCl] = 1.0 M, [$MgCl_2$] = 0.2 M, [HEPES] = 0.1 M, [$ZnCl_2$] = 0.04 M, [oligo(G)] = 1.6–2.6 mM, pH = 8.0. ●, ■, ▲, no poly(C); ○, □, △, [poly(C)] = 0.025 M; ○, ●, 60 °C; □, ■, 80 °C; △, ▲, 100 °C.

Table 4. The Rate Constants (s^{-1} M^{-1}) for the Oligo(G) Hydrolysis at Elevated Temperatures[a)]

T/°C	no poly(C)	0.025 M poly(C)
60	$(1.09 \pm 0.07) \times 10^{-2}$	$(9.38 \pm 0.70) \times 10^{-4}$
80	$(7.41 \pm 0.33) \times 10^{-2}$	$(1.46 \pm 0.03) \times 10^{-2}$
100	$(8.37 \pm 0.44) \times 10^{-1}$	$(6.32 \pm 0.15) \times 10^{-2}$

a) The reaction conditions are the same as shown in Table 1. The reaction curves were fitted using pseudo-second-order model for the hydrolysis of oligo(G).

Discussion

Hydrolysis of ImpG and Oligo(G). Kinetic analyses indicated that the ImpG hydrolysis mainly involves a pseudo-second-order process at 0.04 M Zn^{2+}. This finding is in contrast to the fact that the hydrolysis of imidazole-activated nucleotides catalyzed by Mg^{2+} follows pseudo-first-order kinetics.[69] By hydrolytic studies of the nucleoside 5′-triphosphate, it was confirmed that the hydrolysis obeyed pseudo-second-order kinetics in the presence of metal ions.[67,68] Thus, it is plausible that ImpG hydrolysis is catalyzed by complexation involving two ImpG molecules. The reaction mechanism should be deduced by detail studies on the concentration dependence of Zn^{2+}. Besides, the formation of $G^{5'}$ppG at 0.04 M Zn^{2+} has a similar activation energy (87 kJ mol^{-1}) to that of the ImpG hydrolysis. This fact may indicate that both the ImpG hydrolysis and the formation of $G^{5'}$ppG proceed through a common intermediate.

On the other hand, the hydrolysis of oligo(G) followed a pseudo-second order rate. It has also been known that the hydrolysis of ribonucleotides is catalyzed in the presence of Zn^{2+}.[70–73] In the study, a kinetic analysis of the hydrolysis of dinucleotides showed that the maximum rate was observed at Zn^{2+}/phosphate = 1 : 2.[72] These facts support the pseudo-second-order hydrolysis of oligo(G) in the presence of Zn^{2+}. The fact that both the hydrolyses of ImpG and oligo(G) are consistent with pseudo-second-order processes at 0.04 M Zn^{2+} indicate that the acceleration of the hydrolyses of ImpG and oligo(G) by Zn^{2+} involves a common mechanism.

The hydrolysis of oligo(G) was inhibited in the presence of poly(C) at 60–100 °C. This fact is consistent with the fact that the melting point (T_m) of poly(G)•poly(C) complex is nearly 100 °C,[74–77] which is potentially affected in the presence of metal ions. Actually, it was observed that the absorbance at 250–270 nm gradually increased at 10–70 °C. This is due to the fact that the oligo(G) solution involved different lengths of oligo(G)s, but the T_m value of oligo(G)•poly(C) complex should be lower than that of poly(C)•poly(G) complex, which is nearly 100 °C.[74–77] These facts support that the inhibition of the oligo(G) hydrolysis in the presence of poly(C) at 60–100 °C is due to the partial complexation between oligo(G) and poly(C). In addition, the coincidence between the half-life of the oligo(G) formed by the template-directed reaction and that of the standard oligo(G) in the absence of poly(C) at 60 °C indicates that the hydrolysis of oligo(G) formed by the template-directed reaction followed the hydrolysis in the absence of poly(C).

Oligo(G) Formation with Poly(C) Template at Elevated Temperatures. The formation of higher oligo(G)s at 40–80 °C than that at 37 °C in the previous study[51] is surprising. Further, the high yield of long oligo(G)s indicate that biologically important interactions play effectively at these temperatures. The reason of high efficiency of the formation of long oligo(G)s may be due to that the reaction conditions are somewhat different between the previous and present studies. ImpG was used as an activated-monomer instead of 2-MeImpG and Zn^{2+} was added as a catalyst to form long oligo(G)s in the present study.

The trend in the rate constants of the oligo(G) formation, in which the rate constants increase from 2-mer through 4-mer and then level off, is similar to that of the template-directed reaction of 2-MeImpG at lower temperatures[53] and that of the

spontaneous formation of oligonucleotides in the presence of the montmorillonite clay catalyst.[60,61] This fact indicates that the association between ImpG and elongating oligo(G)s occurs on the poly(C) template, even at 40–60 ˚C. In the present template-directed reaction, a stacking interaction between ImpG and elongating oligo(G) may be promoted in the presence of Zn^{2+}. Actually, it is well known that 3′,5′-linked oligo(G) formed selectively in the presence of Zn^{2+}, which has been considered to be evidence that Zn^{2+} stabilizes the double-helix between poly(C) and ImpG and causes the high regioselectivity of 3′,5′-phosphodiester bond formation.[62] Further, it is surprising that the regioselective formation of 3′,5′-linked oligo(G) at 40–60 ˚C is similar to that observed at lower temperatures.[63] These facts support that the reaction mechanism deduced at lower temperatures[53–59] is able to be applied at 40–60 ˚C.

Besides, the T_m value of ImpG with poly(C) is considered to be much lower than the temperatures used in this study, since the absorbance at 254 nm was less changed at 10–60 ˚C. This fact is consistent with the T_m value of a mixture of 2-MeImpG with poly(C)[78] and that of GMP with poly(C).[79] The fact that the template-directed synthesis is possible at higher temperatures than the T_m of the mixture of activated-monomer and the template. This is interesting because the same trend was also observed in previous studies.[51,78]

There has been less attention on the temperature dependence of the biologically important interactions, such as hydrogen bonding and stacking interaction at elevated to high temperatures. However, the kinetics shown in the study support that interactions between ImpG, growing oligo(G) on the poly(C) template definitely exist at elevated temperatures. The interactions in the present system are probably stronger than those appeared in the template-directed reaction using 2-MeImpG at 37 ˚C in the previous study,[51] since the higher oligo(G)s formed in the present study. Further, it has been discovered that the enhancement of the helix formation between template and oligonucleotides enables the ligation of 2′,5′-linked oligoribonucleotides on a 2′,5′-linked template.[80] Thus, investigations on the association of ImpG with oligo(G) on poly(C) template could be important for a detail analysis of the template-directed reaction in the presence and absence of Zn^{2+}.

The residual amount of poly(C) during the template-directed reaction of oligo(G) was 69% (6 h), 44% (12 h), 37% (18 h), and 31% (24 h) at 60 ˚C and 13% (6 h), 10% (10 h), and 8% (19 h) at 80 ˚C. At these temperatures, the oligomerization reaction was almost completed at 6 h. Therefore, it is deduced that the loss of poly(C) did not notably affect the template-directed formation of oligo(G), but did affect the hydrolytic decomposition of oligo(G).

Comparison of the Formation and Decomposition of Oligo(G). To evaluate the kinetic analysis in the present study, the temperature dependence of the rate constants was evaluated. The Arrhenius plots of the rate constants for the formation of oligo(G), the hydrolysis of ImpG, and the hydrolysis of oligo(G) in the presence and absence of poly(C) are illustrated as a function of T^{-1} (Fig. 6) and the apparent activation energy is determined (Table 5). The rate constants involve some errors, but the Arrhenius plots indicates that the rate constants determined in this study are appropriate to discuss the temperature dependence of the formation and decomposition of oligo(G) using the prebiotic reactions. The rate constants can be compared directly, since all of the reactions follow pseudo-second-order kinetics. The slope for the formation of 3-mer and 4-mer, and that for the ImpG hydrolysis are virtually similar, while the slope of the formation of 2-mer is about 2-times smaller than that of others. The ratio of k_4/k_2 determined by the experiments is 77 (40 ˚C), 158 (50 ˚C), and 233 (60 ˚C), and the estimated k_4/k_2 value from the Arrhenius plots is 660 at 80 ˚C. In addition, the hydrolysis rate of oligo(G) has the largest activation energy among the rate constants in the present template-directed reaction system. The comparison suggests that the 2-mer formation rate is an important factor to determine the yield of oligo(G)s at higher temperatures along with the oligo(G) hydrolysis. The small slope for the 2-mer formation indicates that the associate formation of between two ImpG molecules on poly(C) is more sensitively interfered at higher temperatures than that between ImpG and long oligo(G)s.

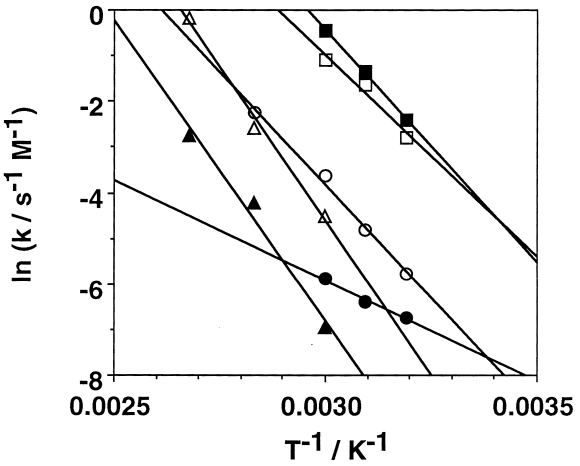

Fig. 6. Arrhenius plots for the template-directed reaction and hydrolysis of ImpG and oligo(G). ○, ImpG hydrolysis; ●, 2-mer formation; □, 3-mer formation; ■, 4-mer and longer formation; △, hydrolysis of oligo(G) in the absence of poly(C); ▲, hydrolysis of oligo(G) in the presence of poly(C).

Table 5. Apparent Activation Energy for the Reactions Relevance to the Template-Directed Oligo(G) Formation

Reactions	E_a/kJ mol^{-1}
ImpG hydrolysis	82
GppG formation	87
Oligo(G) formation	
2-mer	36
3-mer	74
4-mer and longer	85
Oligo(G) hydrolysis	
with poly(C)	112
no poly(C)	109

On the other hand, the apparent activation energy of the hydrolysis of oligo(G) is independent in the presence and absence of poly(C). This fact indicates that the contribution of the entropy change is the main factor of the inhibition of the oligo(G) hydrolysis by the formation of oligo(G)•poly(C) complex.

The temperature dependence of the rate constants is expressed by Eq. II-1–6

$$\ln k_{hy},\text{ImpG} = 25.6 - 9.82 \times 10^3\,T^{-1} \quad \text{(II-1)}$$
$$\ln k_{hy,oligo(G),no\ poly(C)} = 35.7 - 1.34 \times 10^4\,T^{-1} \quad \text{(II-2)}$$
$$\ln k_{hy,oligo(G),with\ poly(C)} = 32.7 - 1.31 \times 10^4\,T^{-1} \quad \text{(II-3)}$$
$$\ln k_2 = 7.28 - 4.40 \times 10^3\,T^{-1} \quad \text{(II-4)}$$
$$\ln k_3 = 25.6 - 8.85 \times 10^3\,T^{-1} \quad \text{(II-5)}$$
$$\ln k_{4av} = 30.2 - 1.02 \times 10^4\,T^{-1} \quad \text{(II-6)}$$

where k_{hy},ImpG is the rate constant of ImpG hydrolysis, $k_{hy,oligo(G),no\ poly(C)}$ and $k_{hy,oligo(G),with\ poly(C)}$ are the rate constants of oligo(G) hydrolysis without and with poly(C), k_2, k_3, and k_{4av} are the rate constants of the formation of 2-mer, 3-mer, and 4-mer and longer. To evaluate whether Eq. II-1–6 provide good reproductions of the experimental data or not, the total amounts of the oligomers of 4-mer and longer determined by the experiments were compared with those calculated using the Eq. II-1–6 at 40–80 ˚C. For the hydrolysis of oligo(G) at 60 ˚C, the rate constants in the presence of poly(C) in the time range 0–2.8 h and those in the absence of poly(C) in the time range 2.8–28 h, respectively. The calculated data (dashed lines in Fig. 4) indicate good agreement with the experimental points. The yield of 4-mer and longer at 80 ˚C was also calculated from the equations, in which a fairly good estimation was performed, even though the equations were determined from the temperature dependence at 40–60 ˚C. Conclusively, these analyses and considerations support the reliability of the rate constants determined by this study and the temperature dependence expressed by Eq. II-1–6.

Importance of the Rate of 2-Mer Formation. The temperature dependence of the rate constant of the formation of 2-mer (Fig. 6) has shown that the rate of 2-mer formation is an important factor to determine the yield of oligo(G). Briefly, the importance of the 2-mer formation rate on the template-directed reaction was pointed out in a previous study.[58] Here, the time course of the extent of oligo(G) was simulated on the basis of the proposed rate constants (Table 3 and 4) and the influence of the k_2 was demonstrated. The simulation was performed using the rate constants at 40 ˚C and a new value of k_2, in which the original k_2 value was multiplied by factors of 1/5, 1/25, 5, or 25. By the simulations, the total concentration of 4-mer and higher (Fig. 7a) and the concentration of 10-mer (Fig. 7b) were visualized. Further, the relationship between the yield of oligo(G) and the oligo(G) length was evaluated (Fig. 7c). The simulations show that the yield of oligo(G) increases with increasing k_2, and that it is highest when the k_2 value is multiplied by a factor of 5. On the other hand, the yield of 10-mer is maximum using the original k_2 value. This relationship is more ambiguously shown in Fig. 7c, in which longer oligomer forms at k_2 = 1/5 and 1/25 than at the original k_2 value. The simulation indicates that the total yield of oligomers does not simply increase with increasing the ratio of k_4/k_2, which is in contrast to the previous prediction.[58]

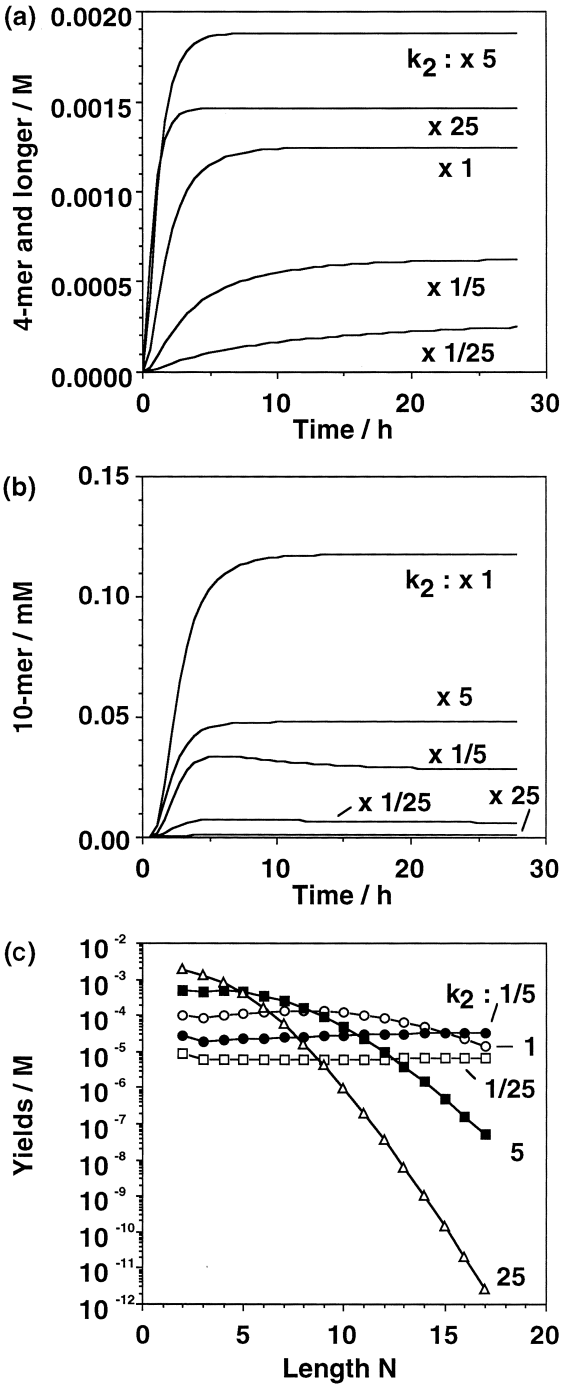

Fig. 7. Computer simulations for the template-directed synthesis using SIMFIT. The rate constants used are of the experimental data of 40 ˚C except 2-mer formation. (a) The total concentration of 4-mer and longer; (b) the concentration of 10-mer; (c) the oligomer concentration vs. length of oligo(G). Different k_2 values are used and the ratios of the k_2 values to the original value are shown.

The simulations support the reliability of the reaction rate constants determined in the study. Further, it has been demonstrated that the k_2 is an important factor to determine the yield

of oligo(G)s and the difficulty of the template-directed formation at higher temperatures is due to decreasing the relative magnitude of the 2-mer formation rate to other pathways.

Conclusions

The present study showed that a template-directed synthesis is possible up to 60 ˚C and that a small amount of oligo(G) forms even at 80 ˚C. In these reactions, the oligo(G) formed by the template-directed reaction is gradually hydrolyzed at 60 ˚C and rapidly at 80 ˚C. The rate constants for the template-directed formation of oligo(G) at 40–60 ˚C were determined. Besides, the kinetics of the hydrolytic degradation of ImpG and oligo(G) suggested that both of the hydrolyses are consistent with pseudo-second-order processes at 0.04 M Zn^{2+}. Based on a comparison of these reaction rates, it was described that the low yield of oligo(G) at 80 ˚C is not only due to the hydrolysis of oligo(G), but also the relatively slow rate of the 2-mer formation.

Thus, these results suggest that a higher yield in the production of oligo(G) would be possible if the degradation of oligo(G)•poly(C) complex can be inhibited and/or the template-directed synthesis can be started using primers longer than 2-mer. In other words, it is concluded that the template-directed formation of RNA from activated monomers was difficult unless the process started with 2-mer or longer, and unless there was some mechanism for protection from the hydrolysis of oligo(G) under hydrothermal environments. The present study and future investigations would provide support to design a RNA world model in vitro, which could have survived under hydrothermal environments.

We thank Professor Taketoshi Nakahara for the use of HPLC apparatus and Dr. Hiroyasu Ogino for the use of UV-vis spectrophotometer in Osaka Prefecture University. Professor G. von Kiedrowski in Ruhr-Universitaet Bochum for generously provided SIMFIT. This research was supported by the Sumitomo Foundation 1998, Japan.

References

1 M.D. Been and T. R. Cech, *Science*, **239**, 1412 (1988).
2 C. Guerrier-Takada, K. Gardiner, T. Marsh, N. Pace, and S. Altman, *Cell*, **35**, 849 (1983).
3 G. F. Joyce, A. W. Schwartz, S. L. Miller, and L. E. Orgel, *Proc. Natl. Acad. Sci. U.S.A.*, **84**, 4398 (1987).
4 T. R. Cech, *Proc. Natl. Acad. Sci. U.S.A.*, **83**, 4360 (1986).
5 W. Gilbert, *Nature*, **319**, 618 (1986).
6 A. A. Beaudry and G. F. Joyce, *Science*, **257**, 635 (1992).
7 "The RNA World," ed by R. F. Gesteland and J. F. Atkins, Cold Spring Harbor Laboratory Press, New York (1993).
8 A. D. Ellington and J. W. Szostak, *Nature*, **346**, 818 (1990).
9 A. Terfort and G. von Kiedrowski, *Angew. Chem., Int. Ed. Engl.*, **31**, 654 (1992).
10 D. Sievers and G. von Kiedrowski, *Nature*, **369**, 221 (1994).
11 H. Yanagawa and F. Egami, *Proc. Jpn. Acad., Ser. B*, **54**, 331 (1978).
12 H. Yanagawa and K. Kojima, *J. Biochem.*, **97**, 1521 (1985).
13 J. A. Baross and S. E. Hoffman, *Origins Life*, **15**, 327 (1985).
14 S. L. Miller and J. L. Bada, *Nature*, **334**, 609 (1988).
15 "Special Issue-Marine Hydrothermal Systems and the Origin of Life," ed by N. G. Holm, *Origins Life Evol. Biosphere*, **22**, 5-242 (1992).
16 W. L. Marshall, *Geochim. Cosmochim. Acta*, **58**, 2099 (1994).
17 N. G. Holm and E. M. Anderson, *Planet Space Sci.*, **43**, 153 (1995).
18 S. W. Fox, *Geochim. Cosmochim. Acta*, **59**, 1213 (1995).
19 E. Imai, H. Honda, K. Hatori, A. Brack, and K. Matsuno, *Science*, **283**, 831 (1999).
20 E. Imai, H. Honda, K. Hatori, and K. Matsuno, *Origin Life Evol. Biosphere*, **29**, 249 (1999).
21 N. R. Pace, *Cell*, **65**, 531 (1991).
22 T. Oshima, *Trans. Mat. Res. Soc. Jpn.*, **19B**, 1069 (1994).
23 T. Oshima, "Seimei ha Nessui kara Hajimatta," Tokyo Kagaku Dojin, Tokyo, (1995).
24 P. Forterre, *C. R. Sciences de la vie/Life sciences, Acad. Sci. Paris*, **318**, 415 (1995).
25 P. Forterre, *Cell*, **85**, 789 (1996).
26 T. Oshima, *Viva Origino*, **25,** 109 (1997).
27 N. Galtier, N. Tourasse, and M. Gouy, *Science*, **283**, 220 (1999).
28 S. L. Miller and A. Lazcano, *J. Mol. Evol.*, **41**, 689 (1995).
29 L. L. Campbell and B. Pace, B. *J. Appl. Bacteriol.*, **31**, 24 (1968).
30 R. H. White, *Nature*, **310**, 430 (1984).
31 Y. Qian, M. Engel, S. A. Macko, S. Carpenter, and J. W. Deming, *Geochim. Cosmochim. Acta*, **57**, 3281 (1993).
32 H. C. Helgeson and J. P. Amend, *Thermochimi. Acta*, **245**, 89 (1994).
33 J. Bada, S. L. Miller, and M. Zhao, *Origins Life Evol. Biosphere*, **25**, 111 (1995).
34 R. Larralde, M. Robertson, and S. L. Miller, *Proc. Natl. Acad. Sci. U.S.A.*, **92**, 8158 (1995).
35 M. Levy and S. L. Miller, *Proc. Natl. Acad. Sci. U.S.A.*, **95**, 7933 (1998).
36 K. Kawamura, A. Yosida, and O. Matumoto, *Viva Origino*, **25**, 177 (1997).
37 K. Kawamura, N. Kameyama, and O. Matumoto, *Viva Origino*, **27**, 107 (1997).
38 K. Kawamura, *Nippon Kagaku Kaishi*, **1998**, 255.
39 K. Kawamura, *Chem. Lett.*, **1999**, 125.
40 K. Kawamura, *Nucleic Acids Symp. Ser.*, **42**, 289 (1999).
41 K. Kawamura, *Bull. Chem. Soc. Jpn.*, **73**, 1805 (2000).
42 R. Lohrmann and L. E. Orgel, *J. Mol. Biol.*, **142**, 555 (1980).
43 T. Inoue and L. E. Orgel, *J. Mol. Biol.*, **162**, 201 (1982).
44 T. Inoue and L. E. Orgel, *Science*, **219**, 859 (1983).
45 L. E. Orgel, *J. Theor. Biol.*, **123**, 127 (1987).
46 H. Sawai, K. Kuroda, and H. Hojo, H. *Bull. Chem. Soc. Jpn.*, **62**, 2018 (1989).
47 H. Sawai, K. Higa, and K. Kuroda, *J. Chem. Soc., Perkin Trans. 1*, **1992**, 505.
48 J. P. Ferris and G. Ertem, *Science*, **257**, 1387 (1992).
49 G. Ertem and J. P. Ferris, *Nature*, **379**, 238 (1996).
50 J. P. Ferris, A. R. Hill, J. R. Liu, and L. E. Orgel, *Nature*, **381**, 59 (1996).
51 H. Fakhrai, T. Inoue, and L. E. Orgel, *Tetrahedron*, **40**, 39 (1984).
52 R. Stribling and S. L. Miller, *J. Mol. Evol.*, **32**, 289 (1991).
53 A. Kanavarioti, C. F. Bernasconi, D. J. Alberas, and E. E.

Baird, *J. Am. Chem. Soc.*, **115**, 8537 (1993).
54 A. Kanavarioti, *Origins Life Evol. Biosphere*, **24**, 479 (1994).
55 A. Kanavarioti, T. B. Hurley, and E. E. Baird, *J. Mol. Evol.*, **41**, 161 (1995).
56 A. Kanavarioti and E. E. Baird, *J. Mol. Evol.*, **41**, 169 (1995).
57 A. Kanavarioti, *J. Org. Chem.*, **63**, 6830 (1998).
58 A. Kanavarioti, C. F. Bernasconi, and E. E. Baird, *J. Am. Chem. Soc.*, **120**, 8575 (1998).
59 A. Kanavarioti, L. F. Lee, and S. Gangopadhyay, *Origins Life. Evol. Biosphere*, **29**, 473 (1999).
60 K. Kawamura and J. P. Ferris, *J. Am. Chem. Soc.*, **116**, 7564 (1994).
61 K. Kawamura and J. P. Ferris, *Origin Life Evol. Biosphere*, **29**, 563 (1980).
62 R. Lohrmann, P. K. Bridson, and L. E. Orgel, *Science*, **208**, 1464 (1999).
63 P. K. Bridson and L. E. Orgel, *J. Mol. Biol.*, **144**, 567 (1980).
64 J. H. G. van Roode and L. E. Orgel, *J. Mol. Biol.*, **144**, 579 (1980).
65 G. F. Joyce, T. Inoue, and L. E. Orgel, *J. Mol. Evol.*, **176**, 278 (1984).
66 J. P. Ferris and G. Ertem, *Origins Life Evol. Biosphere*, **22**, 369 (1992).
67 H. Sigel, F. Hofstetter, R. B. Martin, R. M. Milburn, V. Scheller-Krattiger, and K. H. Scheller, *J. Am. Chem. Soc.*, **106**, 7935 (1984).
68 H. Sigel, *Inorg. Chim. Acta*, **198**–**200**, 1 (1992).
69 A. Kanavarioti, C. F. Bernasconi, D. L. Doodokyan, and D. J. Alberas, D. J. *J. Am. Chem. Soc.*, **111**, 7247 (1989).
70 J. J. Butzow and G. L. Eichhorn, *Biopolymers*, **3**, 95 (1965).
71 J. J. Butzow and G. L. Eichhorn, *Biochemistry*, **10**, 2019 (1971).
72 H. Ikenaga and Y. Inoue, *Biochemistry*, **13**, 577 (1874).
73 J. J. Butzow and G. L. Eichhorn, *Nature*, **254**, 358 (1975).
74 M. N. Lipsett, *J. Biol. Chem.*, **239**, 1256 (1964).
75 M. J. Chamberlin, *Fed. Proc.*, **24**, 1446 (1965).
76 F. Pochon and A. M. Michelson, *Proc. Natl. Acad. Sci. U.S.A.*, **53**, 1425 (1965).
77 D. M. Gray, J.-J. Liu, R. Ratliff, and F. S. Allen, *Biopolymers*, **20**, 1337 (1981).
78 H. T. Miles and J. Frazier, *J. Mol. Biol.*, **162**, 219 (1982).
79 R. J. H. Daves and N. Davidson, *Bipolymers*, **10**, 1455 (1971).
80 H. Sawai, S. Totsuka, K. Yamamoto, and H. Ozaki, *Nucleic Acids Res.*, **26**, 2995 (1998).